Functional Expression of the Na-K-2Cl Cotransporter NKCC2 in Mammalian Cells Fails to Confirm the Dominant-negative Effect of the AF Splice Variant

Membrane Transport, Structure, Function, and Biogenesis:

Functional Expression of the Na-K-2Cl Cotransporter NKCC2 in Mammalian Cells Fails to Confirm the Dominant-negative Effect of the AF Splice Variant

Anke Hannemann, Jenny K. Christie and Peter W. Flatman

J. Biol. Chem. 2009, 284:35348-35358.
doi: 10.1074/jbc.M109.060004 originally published online October 23, 2009

THE JOURNAL OF BIOLOGICAL CHEMISTRY VOL. 284, NO. 51, pp. 35348–35358, December 18, 2009

Functional Expression of the Na-K-2Cl Cotransporter NKCC2 in Mammalian Cells Fails to Confirm the Dominant-negative Effect of the AF Splice Variant*

Received for publication, August 26, 2009, and in revised form, October 6, 2009 Published, JBC Papers in Press, October 23, 2009, DOI 10.1074/jbc.M109.060004

Anke Hannemann, Jenny K. Christie, and Peter W. Flatman[1]

From the Centre for Integrative Physiology, College of Medicine and Veterinary Medicine, The University of Edinburgh, Hugh Robson Building, George Square, Edinburgh EH8 9XD, Scotland, United Kingdom

The renal bumetanide-sensitive Na-K-2Cl cotransporter (NKCC2) is the major salt transport pathway in the apical membrane of the mammalian thick ascending limb. It is differentially spliced and the three major variants (A, B, and F) differ in their localization and transport characteristics. Most knowledge about its regulation comes from experiments in *Xenopus* oocytes as NKCC2 proved difficult to functionally express in a mammalian system. Here we report the cloning and functional expression of untagged and unmodified versions of the major splice variants from ferret kidney (fNKCC2A, -B, and -F) in human embryonic kidney (HEK) 293 cells. Many NKCC2 antibodies used in this study detected high molecular weight forms of the transfected proteins, probably NKCC2 dimers, but not the monomers. Interestingly, monomers were strongly detected by phosphospecific antibodies directed against phosphopeptides in the regulatory N terminus. Bumetanide-sensitive ^{86}Rb uptake was significantly higher in transfected HEK-293 cells and could be stimulated by incubating cells in a medium containing a low chloride concentration prior the uptake measurements. fNKCC2 was less sensitive to the reduction in chloride concentration than NKCC1. Using HEK-293 cells stably expressing fNKCC2A we also show that co-expression of variant NKCC2AF does not have the dominant-negative effect on NKCC2A activity that was seen in *Xenopus* oocytes, nor is it trafficked to the cell surface. In addition, fNKCC2AF is neither complex glycosylated nor phosphorylated in its N terminus regulatory region like other variants.

The Na-K-2Cl cotransporter, isoform 2 (*SLC12A1*; NKCC2)[2] plays key roles in regulating body salt levels and blood pressure (1–3). Located in the apical membrane and subapical vesicles in the thick ascending limb of the Henle loop in the mammalian kidney it is responsible for reabsorbing about 20% of filtered NaCl. In the macula densa it is also essential in tubuloglomerular feedback, the mechanism that matches glomerular filtration to tubular reabsorption. NKCC2 is the clinical target for loop diuretics, defects in its operation cause Bartter disease and its dysregulation may contribute to essential hypertension. Despite its importance relatively little work has been carried out directly on NKCC2 mainly due to difficulties in expressing mammalian NKCC2 in a functionally competent form in mammalian cells (4, 5). Chimeric (6) or tagged (7) versions have been functionally expressed in mammalian cells, as have the native proteins in *Xenopus* oocytes (8, 9), but it is unclear to what extent these reflect the behavior of the native transporter *in vivo*. In addition, although these studies provide important information on transport kinetics and ion affinities (10, 11) they reveal little about transport regulation. Current opinion is based largely through homology on the behavior of closely related NKCC1, which has been successfully expressed and extensively studied (1).

NKCC1 activity is strongly dependent on the phosphorylation of a group of threonine residues in a regulatory domain in its N terminus (Fig. 1*A*) (12, 13). At rest these residues are predominantly unphosphorylated and transport rate is very low. On stimulation, these residues, and in particular that equivalent to Thr^{217} in the human protein, become phosphorylated and the transport rate increases manyfold. One potent stimulus is a fall in cell chloride concentration that causes phosphorylation and activation of SPAK and OSR1, kinases that phosphorylate threonine residues in this regulatory domain (13–16). A very similar motif exists in the N terminus of NKCC2. Recent work shows that ion transport by NKCC2 is affected by phosphorylation or mutation of threonine residues in this motif, and by reduction of cell chloride concentration (17–19). Thus these initial studies suggest aspects of the regulation of NKCC2 are similar to those found with NKCC1, however, essential features remain to be discovered.

Understanding the regulation of NKCC2 is further complicated as the transporter exists in at least 4 splice variants: A, B, and F, which are identical to one another except for a 96-bp exon that encodes for the second transmembrane domain (TM) and part of the first intracellular loop, and AF, which possesses both the A and F exons in tandem (2, 4, 20–23). These differ in their location within the thick ascending limb of the Henle loop and, as the variable region is involved in ion binding, have different affinities for sodium, potassium, and chloride that are appropriate for the composition of urine in part of the thick

* This work was supported by the Wellcome Trust.
⌘ *Author's Choice*—Final version full access.
[1] To whom correspondence should be addressed. Tel.: 44-0-131-3254; Fax: 44-0-131-650-6527; E-mail: peter.flatman@ed.ac.uk.
[2] The abbreviations used are: NKCC, sodium-potassium-chloride cotransporter; SPAK, Ste20-related proline-alanine-rich kinase; OSR1, oxidative-stress response 1; TM, transmembrane; PIC, protease inhibitor cocktail; PBS, phosphate-buffered saline; IPG, immobilized pH gradient; PNGase, *N*-glycosidase F; RACE, rapid amplification of cDNA ends; HEK, human embryonic kidney; CHAPS, 3-[(3-cholamidopropyl)dimethylammonio]-1-propanesulfonic acid.

ascending limb of the Henle loop where they are expressed. Thus NKCC2F, which has the lowest affinity for all three ions, is found exclusively in the medulla, NKCC2A is in both medulla and cortex, and NKCC2B, which has the highest chloride affinity, is exclusively in the macula densa. Both NKCC2A and NKCC2B are involved in tubuloglomerular feedback (24). It is likely that regulation of these variants differs to reflect function, NKCC2F being more involved in mass transport and NKCC2B in signaling. The role of other splice variants, predominant among which is NKCC2AF, is not clear. A role in regulation has been suggested. For instance, although NKCC2AF does not transport ions it has a dominant-negative effect on other NKCC2 variants when co-expressed in oocytes (22).

Here we report the cloning and expression of 4 variants of NKCC2 from ferret (*Mustela putorius furo*) kidney samples (fNKCC2A, -B, -F, and -AF). The material became available during studies on related NKCC1, where the ferret red blood cells was shown to be a powerful functional model (25). Ferrets, like dogs, are members of the order Carnivora and are used to model human physiology in studies of cardiovascular function. We find significantly higher bumetanide-sensitive fluxes in HEK-293 cells transfected with fNKCC2A, -B and -F but not with -AF. Using HEK-293 cells stably expressing fNKCC2A, we demonstrate that the behavior of fNKCC2AF differs significantly from that reported following expression in *Xenopus* oocytes. We also show that many antipeptide antibodies fail to detect expressed fNKCC2 at the expected monomeric molecular weight.

EXPERIMENTAL PROCEDURES

Solutions and Chemicals—All solutions were prepared in Milli-Q water (Millipore, Billerica, MA) using analytical grade chemicals where possible. Unless otherwise stated, the pH was adjusted with NaOH at the appropriate temperature. Lysis buffer comprised (in mM): 50 sodium fluoride, 5 $Na_4P_2O_7$, 5 EDTA, 1 sodium orthovanadate, 1% Triton X-100, 1% protease inhibitor cocktail (PIC, Calbiochem), and 20 HEPES, pH 7.4. Two-dimensional gel electrophoresis lysis buffer (in mM) was: 2 sodium fluoride, 2 $Na_4P_2O_7$, 2 EDTA, 1 sodium orthovanadate, 1% Triton X-100, 1% PIC, 10 Tris-HCl, pH 7.5. PBS was comprised (in mM) of: 137 NaCl, 10 Na_2HPO_4, 1.7 KH_2PO_4, 2.8 KCl.

RNA Isolation and Cloning of Ferret NKCC2—Total RNA was prepared from ferret kidneys stored in RNALater (Qiagen) using the PureLink Micro-to-Midi Total RNA Purification System according to the manufacturer's instructions (Invitrogen). 5′- and 3′-regions of the *slc12a1* gene sequences were obtained using the GeneRacer protocol (Invitrogen). Ferret kidney mRNA was ligated to a GeneRacer RNA-oligo containing known priming sites for subsequent PCRs and reverse transcribed using GeneRacer oligo(dT) primer or random hexamers as primers and SuperScript III reverse transcriptase. 5′- and 3′-RACE (rapid amplification of cDNA ends)-PCR and nested PCR were performed according to the manufacturer's instructions, using GeneRacer primers and gene-specific primers based on conserved regions of known vertebrate *slc12a1* gene sequences (5′ RACE-PCR, 5′-CAG GCA TCC CAT CAC CGT TAG CAA CC-3′; 3′ RACE-PCR, 5′-GAG CTA CCG CCA AGT TCG ACT GAA TGA-3′; 3′ nested RACE-PCR, 5′-GGA AAT CCT CAC AAA GAA CCT CCC TCC T-3′). PCR products were purified, cloned into the pCR4Blunt-TOPO vector, and sequenced (CoGenics, Essex, UK).

The complete open reading frame of the *slc12a1* gene was amplified from the oligo(dT)-transcribed ferret kidney cDNA pool using primers based on our sequence data (sense primer, 5′-GGA AGA TGT TCT CTG AAC AAC ACT T-3′; antisense primer, 5′-CAT GGA TTA AGA GTA AAA TGT CAG TAC-3′). Purified PCR products were cloned into pCR4Blunt-TOPO vector and sequenced. This revealed the presence of four different splice variants, fNKCC2A, -B, -F, and –AF, all of which were subcloned by excision from their respective pCR4Blunt-TOPO construct at the EcoRI sites flanking the polylinker, and ligation into the EcoRI site of mammalian expression vectors pcDNA3.1 (Invitrogen) or pCI-neo (Promega, Madison, WI). Clones were selected for correct orientation of the open reading frame within the construct by colony PCR and subsequently sequenced in both directions. Sequence data have been deposited at GenBank™ under accession numbers GQ338079, GQ338080, and GQ338081 (fNKCC2A, -B, and –F, respectively).

Cell Culture, Transfection, and Stable Cell Lines—HEK-293 cells were maintained in Dulbecco's modified Eagle's medium supplemented with 10% heat-inactivated fetal bovine serum, 100 units/ml of penicillin, 100 μg/ml of streptomycin, and 4 mM L-glutamine. All cells were maintained at 37 °C in a water-saturated atmosphere containing 95% air and 5% CO_2. Cells were split into 6- or 24-well plates the day before transfection. At 60–70% confluence, HEK-293 cells were transfected with the appropriate expression vectors using ExGen 500 (Fermentas, Ontario, Canada) according to the manufacturer's instructions. Stable transfectants were selected by growth in the presence of 0.3 mg/ml of Geneticin (Invitrogen).

^{86}Rb Uptake Studies—24 h after transfection in 6-well plates, HEK-293 cells were subcultured onto poly-D-lysine-coated 96-well plates and grown to confluence for 2 days before the ^{86}Rb uptake assay was carried out. For measurement of ^{86}Rb uptake in stable transfected HEK-293 cells, the cells were plated directly onto poly-D-lysine-coated 96-well plates and grown to confluence for 2–3 days.

Fluxes were measured at room temperature using a modification of a well established method (26). Before each flux assay cells were washed and briefly incubated in basic medium (in mM: 135 NaCl, 2.5 KCl, 1 $CaCl_2$, 1 $MgCl_2$, 5 glucose, 15 HEPES, pH 7.4). Basal fluxes were then measured following further incubation (up to 60 min) in basic medium, whereas stimulated cotransporter fluxes were measured following 2 washes and 60 min of incubation in a hypotonic/low-chloride medium (in mM: 67.5 sodium gluconate, 2.5 potassium gluconate, 0.5 $CaCl_2$, 0.5 $MgCl_2$, 5 glucose, 15 HEPES, pH 7.4). Following these incubations cells were briefly washed in the same incubation medium but with the addition of 0.1 mM ouabain and, where indicated, 10 μM bumetanide. ^{86}Rb uptake was then measured for 3 min (7 min when bumetanide present) in flux medium (in mM: 135 NaCl, 1 RbCl, 1 $CaCl_2$, 1 $MgCl_2$, 5 glucose, 0.1 ouabain, 15 HEPES, pH 7.4). ^{86}Rb uptake was terminated by removing the flux medium and washing cells three times in cold 110 mM $MgCl_2$ using an automatic plate washer (Multiwash III; Tri-

Continent, Grass Valley, CA). Cell ^{86}Rb was determined with a Typhoon PhosphorImager (GE Healthcare). At least 3 wells were used for each experimental point. Cell protein content for each construct was determined from wells that had not received ^{86}Rb. Cells were lysed in lysis buffer and protein concentration was determined using the BCA protein assay (Pierce).

Primary Antibodies—NKCC1-specific antibody (N1) was raised in rabbits to two peptides (^{71}PLGPTPSQSRFQVD^{84} and ^{240}RPSLAELHDELEKEPF^{255}) in the N terminus of human NKCC1 and was affinity purified before use (CovalAb, Villeurbanne, France). The NKCC2-specific antibody (N2-Ct) was generated similarly using a peptide located in the C terminus (^{1005}CKDLTTAEKLKRES^{1018}) of fNKCC2. Other primary antibodies used in this study where either gifts (anti-NKCC2 and anti-pNKCC, D. Alessi (Dundee, UK); R5, B. Forbush (Yale); L224, M. Knepper (National Institutes of Health)) or commercial (T4, Developmental Studies Hybridoma Bank, Iowa City, IA; αNKCC2, Alpha Diagnostics, San Antonio, TX).

Sample Preparation—Protein was isolated from HEK-293 cells ~48 h after transfection using either standard or two-dimensional gel electrophoresis lysis buffer. Crude membrane extracts from ferret and rat kidneys were prepared by homogenization in 250 mM sucrose, 10 mM triethanolamine, 2% PIC followed by sequential centrifugations at 1,000 (10 min) and 17,000 × *g* (20 min). The resulting crude membrane fraction was stored in liquid nitrogen until use. The protein content of all lysates was determined using a BCA protein assay.

Western Blots—Proteins were separated on NuPAGE 3–8% Tris acetate gels (Invitrogen), transferred to polyvinylidene difluoride membranes, and blocked. Blots were incubated with primary antibody in blocking buffer overnight at 4 °C (see Table 1), washed, and incubated with the appropriate horseradish peroxidase-conjugated secondary antibody for 1 h at room temperature. Antibody binding was quantified using Immobilon ECL reagents (Millipore) and Hyperfilm (GE Healthcare) and scanned blots were analyzed with TotalLab (Non Linear Dynamics, Newcastle, UK). Membranes were stripped (62.5 mM Tris-HCl, pH 6.8, 2% SDS) for ~60 min at 70 °C, blocked, and all subsequent steps carried out as described above to reprobe blots with a different antibody. Biotinylated protein ladder (Cell Signaling Technology, Danvers, MA) and MagicMark XP marker (Invitrogen) were used for estimation of molecular weights. For precise work Tris acetate gels were calibrated with both HiMark molecular mass standards (Invitrogen) in the 50–500 kDa range, and biotinylated protein ladder for resultant blots. Comparison of these calibrations allowed more reliable estimation of the molecular weights of the larger complexes.

Two-dimensional Gel Electrophoresis—Samples containing 30–50 μg of protein in two-dimensional gel electrophoresis lysis buffer were prepared in rehydration buffer (final concentration: 7 M urea, 2 M thiourea, 43 mM dithiothreitol, 30 mM Tris base, 1.2% CHAPS, 0.4% amidosulfobetaine-14 (a zwitterionic detergent), 0.25% ampholytes) as described elsewhere (27) and loaded onto 7-cm immobilized pH gradient (IPG) strips (Immobiline DryStrips, pH 3–10, GE Healthcare). First-dimension isoelectric focusing was performed at 20 °C using an IPGphor (GE Healthcare) and the following protocol: 30 min at 0 V, 12 h at 50 V, 4-h gradient to 2000 V, and 6 h at 4000 V. Typically, about 27 kV-h were accumulated during a run. Focused IPG strips were stored at −80 °C until used. Prior to second dimension SDS-PAGE, the strips were defrosted and then incubated for 20 min first in equilibration buffer (6 M urea, 4% SDS, 30% glycerol, 50 mM Tris-HCl (pH 6.8), trace bromphenol blue) containing 25 mM dithiothreitol, and then in equilibration buffer containing 360 mM acrylamide. Second dimension separation was performed on NuPAGE 3–8% Tris acetate gels followed by Western blotting. Protein pI values were estimated from the pH gradient profile of the IPG strip provided by the manufacturer. Theoretical pI values of the proteins were calculated with ProtParam, ExPASy.

Enzymatic Deglycosylation—Cell lysates were incubated with 1% SDS at 60 °C for 20 min and then diluted 5-fold in 71 mM sodium phosphate, pH 7.2, containing 10 mM EDTA, 1% Triton X-100, 1% CHAPS, and 2% PIC. Proteins were deglycosylated by adding 40 units/ml of *N*-glycosidase F (PNGase, Roche) and incubating the lysates overnight at 37 °C. Controls were treated similarly, but without the PNGase.

Cell Surface Biotinylation—48 h after transfection, cells were placed on ice and rinsed twice with ice-cold PBS, pH 7.3, followed by a rinse in borate buffer (in mM: 154 NaCl, 10 boric acid, 7.2 KCl, 1.8 $CaCl_2$, pH 9). Cells were gently agitated for 60 min at 4 °C in borate buffer containing 1.2 mg/ml of Sulfo-NHS-LC-biotin (Pierce). The biotinylation reaction was quenched by three 5-min washes in ice-cold PBS containing 100 mM glycine. Cells were then washed twice in PBS alone, lysed in standard lysis buffer, and the protein concentration determined as described above. Samples containing equal amounts of protein were diluted in lysis buffer and incubated with streptavidin beads (Qiagen) for 1 h at 4 °C under gentle rotation. Supernatant was removed and beads were washed twice in lysis buffer containing 0.5 M NaCl and three times in PBS containing 0.05% Tween 20. Beads were then incubated in sample buffer for 10 min at 40 °C to remove nonspecifically bound proteins. The supernatant was removed and biotinylated proteins were eluted by resuspending the beads in sample buffer and heating them to 100 °C for 10 min.

Statistical Analysis—Values are given as mean ± S.E. and, unless otherwise stated, *n* represents the number of experimental replicates. The difference between means was assessed using two-tailed *t* tests, the level of significance for all tests was set at $p < 0.05$.

RESULTS

Cloning and Sequence Analysis of NKCC2 from Ferret Kidney (fNKCC2)—We cloned the full-length open reading frame of the fNKCC2 mRNA after determining its extreme ends as well as a 251-bp 5′-untranslated region and a 1228-bp 3′-untranslated region via RNA ligase-mediated RACE. Subsequent sequencing of fNKCC2 constructs led to the identification of four variants; fNKCC2A, -B, -F, and -AF (Fig. 1*B*). The predicted masses and pI values of fNKCC2 variants A, B, and F (1100 amino acids) are 121 kDa and 7.7 (AF, 1132 amino acids, 124 kDa, pI 7.9). Sequence alignments with NKCC2s from different species show an overall identity of 95% to mouse, rat, rabbit, and human NKCC2, and 99% to the predicted canine

NKCC2 sequence. The amino acid sequence is 62% identical (~79% similar) to that of the closely related fNKCC1.

Sequence analysis (Fig. 1*A*) shows the presence of the conserved regulatory domain in the N terminus including three threonine residues (Thr[100], Thr[105], and Thr[118]) homologous to the threonine residues phosphorylated in NKCC1 when activated by a reduction in cell chloride concentration or cell volume (12) and the residues (Ser[91], Thr[95], and Thr[100]) homologous to the threonine residues in NKCC1 phosphorylated *in vitro* by SPAK or OSR1 (13). Putative *N*-glycosylation sites Asn[447] and Asn[457] are present in the extracellular domain between TM7 and -8 (28). Two possible SPAK/OSR1 binding sites (15) are present in the N terminus ([20]RFQV[23] and [57]RFRI[60]) but the adjacent protein phosphatase 1 binding site characteristic of NKCC1 (29) is absent.

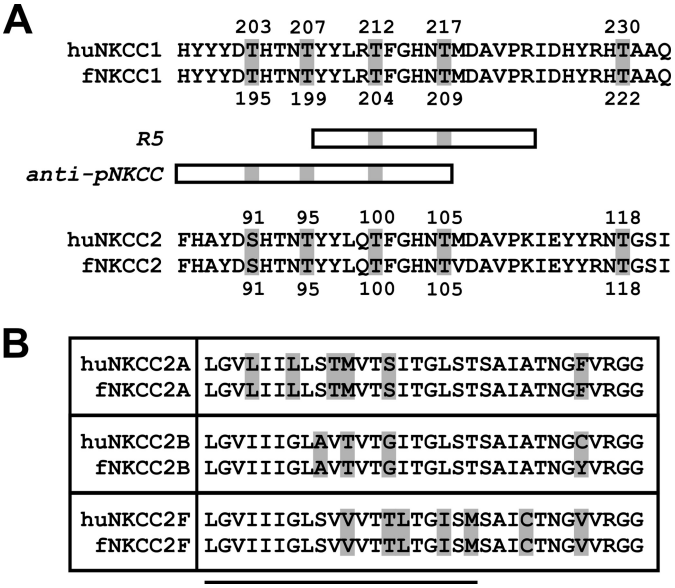

FIGURE 1. **Structural features of fNKCC2.** *A*, regulatory region in the N terminus of NKCC1 and NKCC2. Ferret (*f*) sequences are aligned with their human (*hu*) counterparts. Known phosphorylation sites are marked by *shading*. Peptides used to raise phosphospecific antibodies R5 (30) and anti-pNKCC (13) are shown by *boxes*. *B*, amino acid sequences of fNKCC2 variants are encoded by alternative splicing of the 96-bp cassettes of exon 4. fNKCC2 sequences are aligned with huNKCC2, with differences between the isoforms indicated by shading. The second transmembrane domain is *underlined*.

fNKCC2 Expression in HEK-293 Cells—Our aim was to express fNKCC2 variants in HEK-293 cells and detect the proteins with an NKCC2-specific antibody. In our experience an antibody raised to a fusion protein of the whole cytoplasmic N terminus of NKCC2 (anti-NKCC2, Table 1) gives the most consistent results (see below). As HEK-293 cells express closely related NKCC1, lysates from untransfected cells were used to test for antibody cross-reactivity with endogenous NKCC1 (lane "−" in all blots). NKCC1 is detected by N1 and T4 as bands at ~154 kDa (NKCC1 monomeric weight) and ~316 kDa (possible dimer), whereas phosphospecific R5 (30) mainly detects a band at ~157 kDa, and occasionally a very weak band at ~315 kDa (Figs. 1 and 2 and Table 1).

After transfecting HEK-293 cells with fNKCC2A, -B, -F, and -AF constructs, whole cell lysates were tested for the presence of fNKCC2 using a variety of antibodies (Fig. 2, *A* and *B*, and Table 1). Anti-NKCC2 detected strong bands at the expected monomeric mass of glycosylated NKCC2, ~134 kDa, in cells transfected with fNKCC2A, -B, and -F, but not following transfection with fNKCC2AF. It also detected bands at ~104 kDa with all four constructs (Fig. 2*A*), perhaps indicating that the substantial unglycosylated or poorly glycosylated transporter is produced in these transiently transfected cells. However, all other NKCC2 antibodies except L224 (and in this case only with large samples of A, B, or F) failed to detect the low molec-

TABLE 1

Detection of NKCC1 and NKCC2 by various antibodies

Molecular masses were estimated on scanned blots with TotalLab software. Molecular masses are mean ± S.D. (n ≥ 4 in most cases, values based on a single observation indicated by ~) (aa, amino acid; hu = human; f = ferret; r = rat).

Antibody	Immunogen and targets in some equivalent proteins	Bands detected		
		HEK-293	Transfected with fNKCC2 variant[a]	
			Monomer molecular mass	High molecular mass
		kDa		
N1	N terminus, 2 peptides, huNKCC1, aa 71–84 and 235–255	317 ± 11 154 ± 3		
T4	Last 310 aa of C terminus, huNKCC1, monoclonal	316 ± 10 154 ± 4		277 ± 7 (A, B, F) 238 ± 4 (A, B, AF)[b] 222 ± 4 (F)[b]
R5	Phospho-peptide, huNKCC1, aa 208–223 (Thr(P)[212], Thr(P)[217]) (fNKCC1: Thr(P)[204], Thr(P)[209]; fNKCC2: Thr(P)[100], Thr(P)[105])	157 ± 5	135 ± 5 (A, B, F)	279 ± 7 (A, B, F)
Anti-pNKCC	Phospho-peptide, huNKCC1, aa 198–217 (Thr(P)[203], Thr(P)[207], Thr(P)[212]) (fNKCC1: Thr(P)[195], Thr(P)[199], Thr(P)[204]; fNKCC2: Ser(P)[91], Thr(P)[95], Thr(P)[104])	~155	~134 (A, B, F)	~275 (A, B, F)
Anti-NKCC2	Entire cytoplasmic N terminus, huNKCC2	~315[c]	134 ± 4 (A, B, F) 104 ± 4 (all)	273 ± 8 (A, B, F) 233 ± 4 (A, B, AF)[b] 220 ± 5 (F)[b]
L224	N terminus, peptide, rNKCC2, aa 109–129		~134 (A, B, F)[d]	275 ± 4 (A, B, F) ~235 (A, B, AF)[d], ~222 (F)[d]
N2-Ct	C terminus, peptide, fNKCC2, aa 1045–1018			279 ± 1 (A, B, F) 237 ± 2 (A, B, AF)[d], ~222 (F)[d]
αNKCC2	C terminus, rNKCC2, 15 aa peptide			277 ± 1 (A, B, F) 234 ± 2 (A, B, AF)[b], ~222 (F)[b]

[a] Only additional bands tabulated also have bands found in HEK-293 controls.
[b] Present in most blots.
[c] Cross-reactivity seen if blots are overloaded and overexposed.
[d] Present in minority of blots and only after long exposure times.

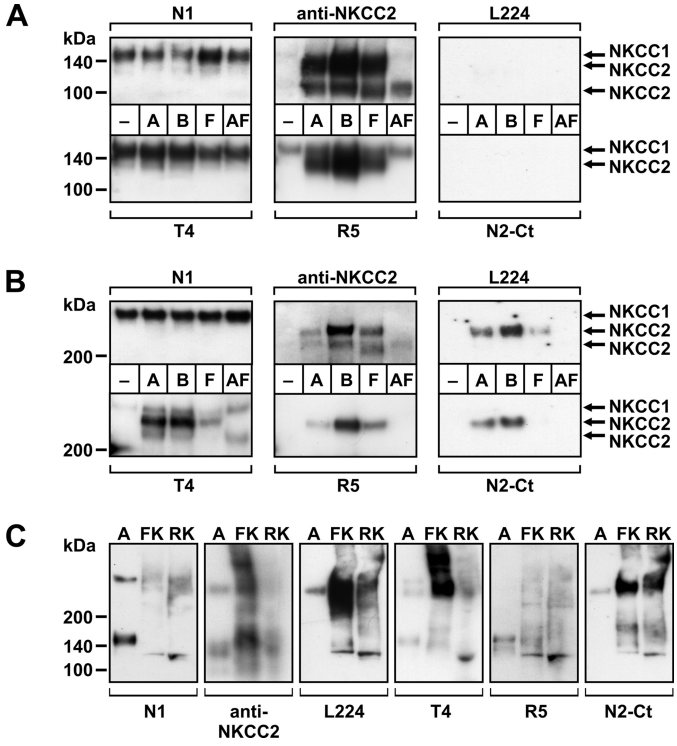

FIGURE 2. **Interaction of fNKCC2 variants with antibodies.** *A* and *B*, whole cell lysates (7 μg) of untransfected (−) HEK-293 cells and cells transfected with fNKCC2A, -B, -F, and -AF; and *C*, crude membranes (adjusted to allow similar levels of detection) from ferret (*FK*) and rat (*RK*) kidneys, were subjected to SDS-PAGE and immunoblotted with antibodies (see Table 1 for details) against NKCC1 (*N1*), NKCC2 (*anti-NKCC2*, *L224*, and *N2-Ct*), NKCC1 and 2 (*T4*), and phoshpo-NKCC1 and 2 (*R5*). Molecular mass markers (in kDa) are shown on the *left* and NKCC isoforms on the *right*. *A*, monomeric NKCC. *B*, high molecular weight bands. The molecular weight calibration in the *top* and *bottom panels* are identical. *C*, comparison of NKCCs in kidney and fNKCC2A-transfected HEK-293 cells.

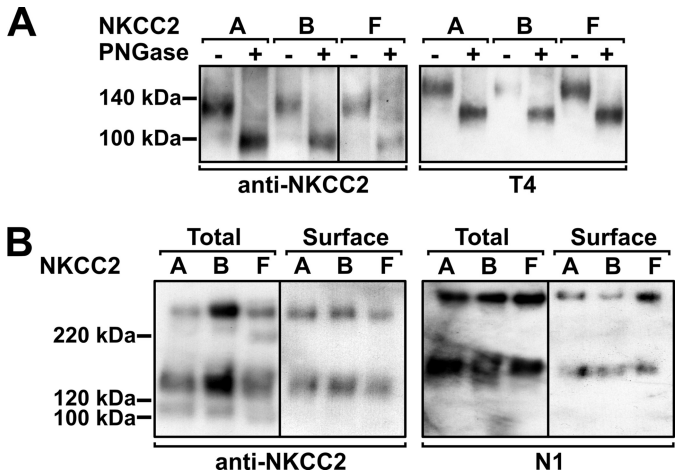

FIGURE 3. **fNKCC2 glycosylation and appearance in the cell surface.** *A*, whole cell lysates from HEK-293 cells transfected with fNKCC2A, -B, and -F were treated with (+) or without (−) PNGase F, subjected to SDS-PAGE, and immunoblotted with anti-NKCC2 (*left panel*) and re-probed with T4 (*right panel*). Exposure time was increased to detect fNKCC2F (shown by *vertical line*). *B*, detection of surface proteins. 48 h after transfection HEK-293 cells were surface biotinylated with Sulfo-NHS-LC-biotin. Biotinylated proteins were precipitated from cell lysates with streptavidin beads, eluted, run on SDS-PAGE, and immunoblotted with anti-NKCC2 (*left panels*) and re-probed with N1 to detect endogenous NKCC1 (*right panels*). Twice as much protein was loaded and longer exposure times were used to detect surface proteins compared with total proteins. Molecular mass markers (in kDa) are indicated.

ular weight forms of fNKCC2 (Fig. 2*A* and Table 1) despite the epitopes being present with, at most, only minor modification. On the other hand these same NKCC2 antibodies detected high molecular weight forms of expressed fNKCC2 (Fig. 2*B* and Table 1). Interestingly, the phospho-specific antibody R5 detected additional bands at both ~135 (Fig. 2*A*) and ~279 kDa (Fig. 2*B*) in NKCC2A, -B, and -F (but not -AF) transfected cells, and a phospho-specific antibody raised to an adjacent epitope (anti-pNKCC; Fig. 1*A* and Table 1) showed the same band pattern.

As no significant differences were seen in the molecular weights of the principal bands detected by the different antibodies, data can be combined. Transfection of HEK-293 cells with fNKCC2A, -B, or -F causes the appearance of additional bands at (average molecular masses) 104, 134, and 275 kDa. A band that appears at 235 kDa in fNKCC2A or -B runs at 222 kDa in fNKCC2F. Expression of fNKCC2AF causes bands to appear at 104 and 235 kDa. Normally, anti-NKCC2 did not detect endogenous NKCC1. However, with very long exposures (for instance, when being used to detect variant -AF), a faint band at the characteristic weight of NKCC1 could be detected (Fig. 6*A*). In contrast, we found no evidence for cross-reaction between N1 and fNKCC2 even when expressed at high levels. In addition, independent of the antibody used, we generally found that for the same protein load, lysates of cells transiently transfected with fNKCC2B gave approximately twice as much signal as those transfected with fNKCC2A, which in turn was twice as much as with fNKCC2F.

To see if difficulties in detecting the monomeric forms of fNKCC2 were merely a problem of the expression system or the species used, we probed crude membrane preparations of ferret and rat kidney with the same set of antibodies, using lysates of HEK-293 cells transfected with fNKCC2A for comparison (Fig. 2*C*). Again, T4, L224, and N2-Ct detected strong high molecular weight bands but also detected at least one band at the approximate monomeric weight of NKCC2. A greater proportion of NKCC2 was found in high molecular weight forms in ferret compared with rat samples. Interestingly, N1 detected bands at the same molecular weights (lower than NKCC1 in other tissues), suggesting kidney NKCC1 and NKCC2 migrate similarly on SDS-polyacrylamide gels.

fNKCC2 Is Heavily Glycosylated and Trafficked to the Cell Surface—To be functional both NKCC1 and NKCC2 are heavily glycosylated on two asparagine residues in the extracellular loop between TM7 and -8 (1, 28). As these residues are conserved in fNKCC2 (Asn^{447} and Asn^{457}) we examined the effects of treating cell lysates with PNGase (Fig. 3*A*). The *right-hand panels* of Fig. 3*A* show that the apparent molecular mass of endogenous NKCC1 falls by ~30 kDa when deglycosylated. The fall is similar whether the cells were transfected with fNKCC2A, -B, or -F. The apparent mass of monomeric fNKCC2 (*left-hand panel*, Fig. 3*A*) falls by about 35 kDa (to ~99 kDa) supporting the idea that the 104-kDa band represents poorly or unglycosylated fNKCC2. Although similar results were obtained with the higher molecular weight forms of NKCC1, the decrease in apparent molecular mass for NKCC2 was larger (~45 kDa, data not shown), suggesting that the 275-kDa bands represent complex glycosylated forms, and the 235

(or 222)-kDa bands represent poorly or unglycosylated forms. Comparison with Fig. 2 indicates that only the complex-glycosylated forms (134 and 275 kDa) can be phosphorylated and detected by phospho-specific antibodies like R5.

To see if the fNKCC2 isoforms were properly trafficked to the plasma membrane we biotinylated surface proteins by reaction with sulfo-NHS-LC-biotin and precipitated biotinylated proteins with streptavidin beads. Endogenous NKCC1 and exogenous fNKCC2 were then identified by Western blotting with specific antibodies (Fig. 3*B*). Monomeric and high (possibly dimeric) molecular weight forms of both NKCC1 and fNKCC2 could be biotinylated at the cell surface suggesting they are trafficked to the plasma membrane. There was no difference between fNKCC2A, -B, and -F and, as has been described before (7), only the complex-glycosylated forms (bands at 134 and 275 kDa, but not at 104, 235, or 222 kDa, Fig. 3*B*) of the cotransporter appeared in the biotinylated fraction. As larger sample sizes and longer exposure times were required to detect the transporters in the biotinylated compared with whole cell samples it appears that only a small fraction of total NKCC1 or fNKCC2 is in the surface membrane and can be biotinylated as suggested previously (31, 32).

Expressed fNKCC2 Is Functional—After confirming fNKCC2 was expressed, complex glycosylated, and trafficked to the plasma membrane, we next tested if it was functional by measuring the bumetanide-sensitive uptake of ^{86}Rb under two conditions. First, after a 1-h incubation in an isotonic medium to assess basal cotransporter activity, and second, after 1 h in a hypotonic/low-chloride medium to activate the cotransporter. The fluxes themselves were measured in identical media. Transfection of HEK-293 cells with empty vector had no effect on fluxes under either condition (Fig. 4). Robust additional bumetanide-sensitive ^{86}Rb uptakes were observed in cells transfected with fNKCC2A, -B, and -F incubated under isotonic conditions. These basal fluxes showed the largest proportional increase following transfection. Compared with untransfected cells, basal activity was increased by 80% with fNKCC2A, 140% with fNKCC2B, and 50% with fNKCC2F (Fig. 4). Interestingly, this roughly follows the observed relative expression levels of fNKCC2A, -B, and -F in HEK-293 cells (Fig. 2). Even though these increases in ^{86}Rb uptake are highly significant ($p < 0.005$), 30–40% of bumetanide-sensitive ^{86}Rb uptakes probably occur through the endogenous NKCC1 of the HEK whose expression level and phosphorylation state (Fig. 2*A*) are not affected by the expression of any fNKCC2 variant. Bumetanide-resistant ^{86}Rb fluxes were not significantly affected by transfecting HEK-293 cells with fNKCC2 variants, nor were they affected by incubating these cells in a hypotonic/low chloride medium (103.6 ± 2.7% control, $n = 7$).

The highest fluxes were measured following incubation in hypotonic/low-chloride medium to stimulate NKCC2 (18). However, transfecting cells with fNKCC2A and -B caused a smaller relative increase in bumetanide-sensitive ^{86}Rb uptake under these conditions (40% for fNKCC2A and 80% for fNKCC2B) compared with results obtained under isotonic conditions, although the increase for fNKCC2F (50%) was similar to that under isotonic conditions. Although ^{86}Rb uptakes were significantly higher in transfected cells, this result shows that

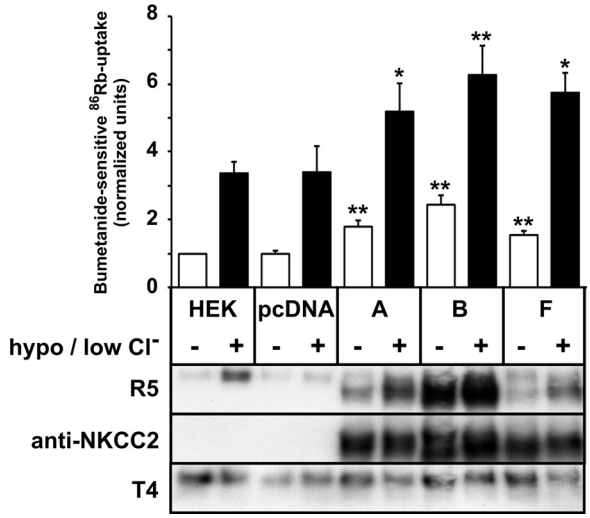

FIGURE 4. **Functional expression of fNKCC2 variants in HEK-293 cells.** HEK-293 cells were transfected with empty vector (*pcDNA*) or fNKCC2 constructs (*A*, *B*, and *F*) and grown to confluence. 2–3 days post-transfection, ^{86}Rb uptake was assessed following preincubation in isotonic (basal conditions, *open bars*) or hypotonic/low-chloride medium (*filled bars*). In each experiment, ^{86}Rb uptakes were normalized to the ^{86}Rb uptake in untransfected HEK-293 cells under basal conditions and shown as mean ± S.E. Uptake (in nanomole mg protein^{-1} min^{-1}) under basal conditions were 4.0 ± 0.4 ($n = 19$) and in specific experiments were: 4.7 ± 0.8 (*versus* pcDNA), 4.2 ± 0.6 (*versus* fNKCC2A), 4.1 ± 0.5 (*versus* fNKCC2B), and 3.6 ± 0.5 (*versus* fNKCC2F). Transfection of HEK-293 cells increased bumetanide-sensitive ^{86}Rb uptake by 80 ± 17% (-*A*, $n = 9$), 144 ± 26% (-*B*; $n = 10$), and 53 ± 13% (-*F*; $n = 10$) under basal conditions and by 39 ± 10% (-*A*, $n = 5$), 82 ± 6% (-*B*, $n = 5$), and 50 ± 6% (-*F*, $n = 5$) following incubation in a hypotonic/low-chloride medium. *, $p < 0.05$; **, $p < 0.005$ compared with HEK-293 uptake under the same condition. Uptakes in the presence of 10 μM bumetanide were similar under all conditions. Thus between 14 and 35% total uptake was bumetanide-insensitive depending on whether the cells had been incubated in hypotonic/low chloride or isotonic media. Expression and phosphorylation of NKCC proteins were assessed by immunoblot analysis using the antibodies indicated.

pre-treatment with hypotonic/low-chloride medium causes greater activation of endogenous NKCC1 than transfected fNKCC2. In all cases, stimulation by hypertonic/low-chloride pre-treatment was accompanied by an increase in phosphorylation of the regulatory threonine residues in the N termini of the transporters as detected by R5 (Fig. 4), whereas endogenous NKCC1 and fNKCC2 protein levels remained constant (Fig. 4).

Stable Expression of fNKCC2—To date, the only report of a cell line stably expressing NKCC2 concerns a NKCC1–NKCC2 chimera in which the first 104 amino acids of rabbit NKCC2A had been replaced by the equivalent residues of human NKCC1 (6). After observing functional fNKCC2 expression in transient transfected cells, we also tried to create stable cell lines. Following selection for geneticin resistance, cells were tested for the presence of the fNKCC2 protein. As shown in Fig. 5*A*, a strong NKCC2 signal was detected in cells transfected with fNKCC2A, whereas those from cells expressing fNKCC2B and -F were much weaker, and none was seen in cells transfected with empty vector. The strength of the NKCC1 signal was similar with all variants (Fig. 5*A*, *bottom panel*) indicating that the stable expression of fNKCC2 does not affect the total level of NKCC1 in these cells. Functional expression of fNKCC2 was assessed by measuring bumetanide-sensitive ^{86}Rb uptake in cells under isotonic conditions or following incubation in hypotonic/low-chloride medium. Stable expression of the empty

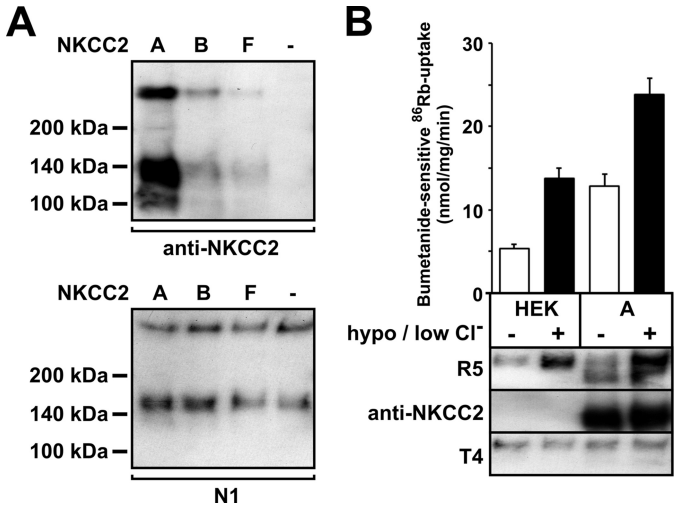

FIGURE 5. **Stable expression of fNKCC2.** *A,* HEK-293 cells were transfected with pCI-fNKCC2 constructs (*A*, *B*, and *F*) or empty vector (−) and selected for geneticin resistance. Equal amounts of whole cell lysates were subjected to SDS-PAGE, immunoblotted with anti-NKCC2 (*top panel*), and re-probed with N1 (*bottom panel*). Molecular size markers (in kDa) are indicated. *B,* HEK-293 cells either untransfected, or stably expressing fNKCC2A, were grown to confluence, and ^{86}Rb uptake was assessed following incubation of cells in isotonic (basal conditions, *open bars*) or hypotonic/low-chloride (*filled bars*) medium. Bumetanide-sensitive ^{86}Rb uptakes are shown as mean ± S.E. Stable expression of fNKCC2A increased ^{86}Rb uptake by 145 ± 30% (n = 17, p = 0.00028) in basal conditions and by 72 ± 10% (n = 16, p = 0.00013) following incubation in hypotonic/low-chloride medium. Expression and phosphorylation of NKCC proteins were assessed using the antibodies indicated.

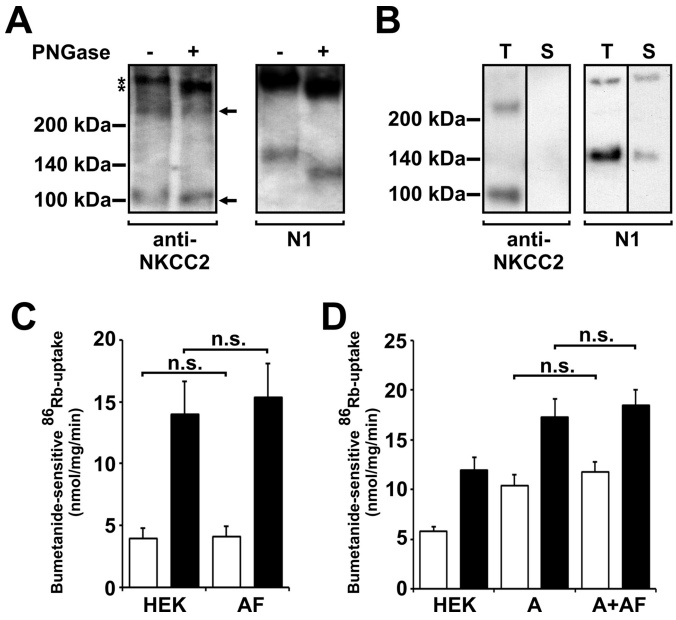

FIGURE 6. **fNKCC2AF: glycosylation, surface expression, and ^{86}Rb uptake.** *A*, cell lysates from HEK-293 cells transfected with fNKCC2AF were incubated with (+) or without (−) PNGase F, subjected to SDS-PAGE, immunoblotted with anti-NKCC2 (*left panel*), and re-probed with N1 antibody (*right panel*). Molecular size markers (in kDa) and cross-reaction of anti-NKCC2 with NKCC1 (*) are indicated on the *left* and NKCC2AF is marked by an *arrow on the right*. *B*, 48 h after transfection with fNKCC2AF HEK-293 cells were surface biotinylated with Sulfo-NHS-LC-biotin. Biotinylated proteins were precipitated from cell lysates with streptavidin beads, run on SDS-PAGE, immunoblotted with anti-NKCC2 (*left*), and re-probed with N1 to detect endogenous NKCC1 (*right*). Twice as much protein was loaded and longer exposure times were used to detect surface proteins (*S*) compared with total proteins (*T*). *C*, untransfected (*HEK*) and fNKCC2AF-transfected (*AF*) HEK-293 cells, and *D*, stable fNKCC2A (*A*) and stable fNKCC2A cells co-expressing fNKCC2AF (*A*+*AF*) were grown to confluence (2–3 days). ^{86}Rb uptake was assessed following incubation of cells in isotonic (basal conditions, *open bars*) or hypotonic/low-chloride (*filled bars*) medium. Bumetanide-sensitive ^{86}Rb uptakes are shown as mean ± S.E. Expression of fNKCC2AF has no significant (*n.s.*) effect on ^{86}Rb uptakes by HEK-293 cells (*C*) ($n \geq 4$) or HEK-293 cells stably expressing fNKCC2A (*D*) ($n \geq 3$).

vector did not significantly affect fluxes under these conditions (relative to control HEK-293: 110 ± 7% (isotonic, n = 7) and 103 ± 8% (hypotonic/low-chloride, n = 5)). Stable expression of fNKCC2A caused a significant increase in ^{86}Rb uptake under both conditions (Fig. 5*B*) with uptake increased by 145 and 72% following incubation in isotonic or hypotonic/low-chloride media, respectively. As with cells transiently expressing fNKCC2A, activation was less following preincubation in hypotonic/low-chloride medium. In contrast, no significant changes in ^{86}Rb uptakes were found in cells stably expressing fNKCC2B or -F under either condition (data not shown). This is most likely due to low expression of these fNKCC2 variants as demonstrated by the Western blots (Fig. 5*A*).

fNKCC2AF Does Not Affect Transport by fNKCC2A—NKCC2AF has only previously been expressed and characterized in oocytes (5, 22), and we now demonstrate that it can also be transiently expressed in HEK-293 cells. Fig. 2, *A* and *B* (*lanes AF*), show that anti-NKCC2 detects the 104- and 235-kDa bands and T4 the 235-kDa band in HEK-293 cells expressing fNKCC2AF. As this pattern is characteristic of poorly glycosylated forms of other NKCC2 variants (Fig. 3*A*) we suggest that fNKCC2AF is not properly glycosylated by the cell. This view is supported by the finding that treatment of lysates of cells transfected with fNKCC2AF with PNGase did not cause any significant change in the molecular weight of bands detected with anti-NKCC2 (Fig. 6*A*, *left*), whereas the expected reduction of 30 kDa was seen in bands detected with N1 (NKCC1, Fig. 6*A*, *right*).

Expressed fNKCC2AF does not appear to be trafficked to the cell surface. Proteins with extracellular domains in fNKCC2AF-expressing cells were biotinylated and then isolated using streptavidin beads. When subjected to Western blotting these proteins did not react with anti-NKCC2 although they did with N1 (NKCC1) (Fig. 6*B*). Both NKCC1 and fNKCC2AF were detected in whole cell lysates from these cells (Fig. 6*B*). In addition, transient transfection of HEK-293 cells with fNKCC2AF did not affect bumetanide-sensitive ^{86}Rb uptake measured under basal conditions or following preincubation in an hypotonic/low-chloride medium (Fig. 6*C*).

It has been reported that expression of NKCC2AF in oocytes has a dominant-negative effect on coexpressed NKCC2A or -F (22). To see whether this also occurs in the HEK-293 cell expression system, we transfected HEK-293 cells stably expressing fNKCC2A with fNKCC2AF and measured the resulting bumetanide-sensitive ^{86}Rb uptakes under basal conditions and following preincubation in hypotonic/low-chloride medium. Fig. 6*D* shows that ^{86}Rb uptakes by cells stably expressing fNKCC2A were not affected by the co-expression of fNKCC2AF under either condition. There is no evidence for a dominant-negative effect in the HEK-293 cell system.

Two-dimensional Electrophoresis of fNKCC2 and NKCC1—NKCC1 and NKCC2 may have similar molecular weights as determined by SDS-PAGE (especially if unglycosylated forms

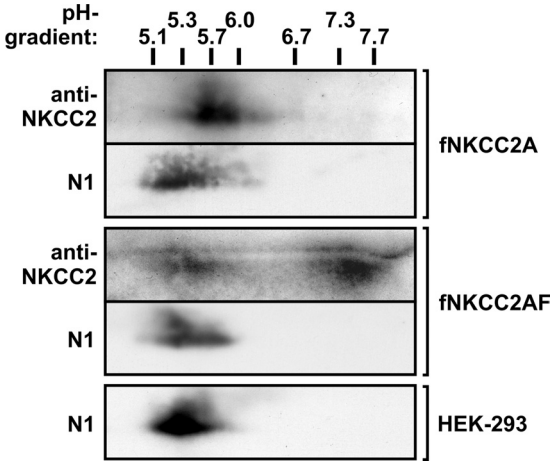

FIGURE 7. **Comparison of NKCC1 and fNKCC2 by two-dimensional gel electrophoresis.** Whole cell lysates from untransfected, fNKCC2AF-transfected HEK-293 cells, and cells stably expressing fNKCC2A were separated on 7-cm Immobiline DryStrips pH 3–10, the strips were subjected to SDS-PAGE followed by immunoblotting with anti-NKCC2 and re-probing with N1 antibody. Representative blots are shown. The molecular masses of complexes exceeded 300 kDa. The pH gradient across the strip, calculated according to information provided by the manufacturer, is given at the *top*.

are present) and identification via Western blotting can be hindered by cross-reactions of available antibodies. However, as their theoretical pI values differ widely (fNKCC1, pI = 6.1; fNKCC2, pI = 7.7), better discrimination between the isoforms might be achieved using two-dimensional gel electrophoresis. Whole cell lysates of HEK-293 cells and HEK-293 cells transfected with fNKCC2A were subjected to isoelectric focusing on immobilized pH gradients as the first dimension, and SDS-PAGE as the second. Endogenous NKCC1 and fNKCC2A were found as high-molecular mass (~300 kDa) complexes with broad overlapping pI values (Fig. 7) ranging from pH 5.1 to 6.1 for NKCC1 and pH 5.4 to 6.4 for fNKCC2A. However, the majority of NKCC1 was detected between pH 5.25 and 5.65, whereas the majority of fNKCC2A appeared between pH 5.5 and 5.95, revealing a small but distinct difference in the pI ranges of the two isoforms. Post-translational modifications can have a strong influence on protein pI and both glycosylation and phosphorylation would be expected to move the pI values in the acidic direction as observed. However, we were surprised that the large difference in (theoretical) pI values was so greatly attenuated. This was mainly due to the pI of fNKCC2A, which had become much more acidic than expected. We repeated the experiment with samples containing fNKCC2AF as this is neither glycosylated (Fig. 6*A*), nor phosphorylated in the N terminus regulatory domain (Fig. 2, *A* and *B*). Anti-NKCC2 detected two distinct signals. One signal, probably representing fNKCC2AF itself, stretched from pH 6.9 to 7.7 with the strongest signal between pH 7.35 and 7.7 and a second signal was detected from pH 5.3 to 5.8. The latter corresponds to the most intense area of the N1 signal (Fig. 7, *fourth panel*) and is most likely caused by cross-reaction of anti-NKCC2 with NKCC1 when long exposures are used (see Fig. 6*A*). Thus, the observed pI for fNKCC2AF is much closer to its theoretical value than that of fNKCC2A demonstrating the extent of post-translational modifications on fNKCC2A. No differences could be detected in the pI values of NKCC1 in untransfected HEK-293 cells (Fig. 7, *bottom*) and in those expressing either fNKCC2A or -AF making it unlikely that NKCC1 forms heterodimers with fNKCC2.

DISCUSSION

To study the regulation of NKCC2 it is important that unmodified forms of NKCC2 be expressed in a mammalian system. Small changes in the structure of NKCC2, for instance, phosphorylation or a change in the hydrophobicity of just a few residues, can have a large impact on function, altering activity, trafficking, or propensity to bind regulators. The addition of small tags that permit expression (as was necessary in the past) may also alter its responses to stimuli. In this paper we demonstrate for the first time the functional expression of the major NKCC2 variants, fNKCC2A, -B, and -F in mammalian HEK-293 cells. We used native proteins that had not been tagged or modified in any other way. Our results also help explain why functional expression of NKCC2 was so problematic in the past. It resulted from three factors: poor reactivity of expressed NKCC2 with available antibodies, the small size of fluxes through transfected NKCC2, and the expectation that a reduction in cell chloride concentration would help reveal the presence of the transporter.

Our studies show that expressed fNKCC2A, -B, and -F become glycosylated (Fig. 3) and can be phosphorylated in the regulatory threonine domain in their N termini (see Figs. 2 and 4). Unglycosylated forms are not phosphorylated (Fig. 2), nor do they appear in the plasma membrane (see Figs. 3 and 6). Bumetanide-sensitive fluxes in transfected cells are about twice the size of fluxes through the endogenous (NKCC1) system in control (untransfected, mock-transfected) cells under basal conditions (see Fig. 4). With transient transfection the magnitudes of these fluxes follow the order B > A > F, which follow the intensities of expressed fNKCC2 protein (see Fig. 2). Fluxes in transfected cells are stimulated more than 2-fold by preincubating them in hypotonic/low-chloride medium and are substantially greater than fluxes in untransfected HEK-293 cells under the same conditions (Fig. 4). As this preincubation causes maximal activation of endogenous NKCC1 it is likely that the additional fluxes seen in transfected cells are mediated by NKCC2 and are not due to stimulation of endogenous transporters. It also seems unlikely that transfected fNKCC2 takes over the role of endogenous NKCC1 as the expression of fNKCC2 affects neither the levels nor phosphorylation status of endogenous NKCC1 (Fig. 4).

Stable transfections with fNKCC2A, -B, and -F were also achieved. High levels of transfected proteins were obtained for fNKCC2A but the levels were much lower for fNKCC2B and -F (Fig. 5). We show that fNKCC2A is functional in stable cells with bumetanide-sensitive ^{86}Rb fluxes that are larger than in transiently transfected cells (12.9 ± 1.4 (*n* = *19*) *versus* 6.9 ± 1.3 (*n* = *8*) nmol mg protein^{-1} min^{-1}, respectively, Figs. 4 and 5). However, although additional fluxes could be detected in stable fNKCC2B and -F cells these did not reach statistical significance. This was not surprising given the low level of transfected proteins and the level of background, NKCC1-mediated fluxes. Others have had a similar experience with the only other NKCC2 construct that has been successfully stably expressed in

mammalian cells, an NKCC1–NKCC2A chimera (6). This construct produced robust fluxes, whereas similar chimeras containing NKCC2B or -F did not. It is striking that very small variations in the TM2 structure of NKCC2 and intracellular loop 1 have such a large impact on the ability of HEK-293 cells to stably express the transporter. This might be due to the differences in ion affinities and the effects these have on transport under culture conditions. Alternatively, they may affect interactions between transporter and vital regulatory molecules. Some of these problems might be overcome by using an inducible gene expression system to allow the establishment of stable cell lines before expression of the transporters.

We also expressed fNKCC2AF in HEK-293 cells (Fig. 6). Western blotting showed that although the protein was readily detected it was not surface biotinylated, nor did it become glycosylated or phosphorylated in the N terminus, a view supported by two-dimensional gel electrophoresis experiments (Fig. 7), which also suggested that fNKCC2AF exists in the cell as a high molecular weight complex (possible dimer). Bumetanide-sensitive ^{86}Rb fluxes in these cells were identical to fluxes in untransfected HEK-293 cells. As we find fNKCC2AF is not trafficked to the cell surface our uptake results do not indicate whether fNKCC2AF can transport ions, although studies on *Xenopus* oocytes suggest it does not (22). Importantly, the transient expression of fNKCC2AF had no effect on the bumetanide-sensitive ^{86}Rb fluxes in cells stably expressing fNKCC2A under basal conditions or after preincubation in hypotonic/low-chloride medium. Together, these experiments suggest that fNKCC2AF does not affect either the trafficking of, or fluxes through, endogenous NKCC1, or stably expressed fNKCC2A. No evidence could be found for a dominant-negative effect for this variant in the mammalian expression system. This contrasts with the situation in *Xenopus* oocytes where NKCC2AF (from shark) was detected in the plasma membrane and reduced flux through co-expressed NKCC2A or -F (22). This is reminiscent of the contrasting ways in which *Xenopus* oocytes and mammalian cells process cystic fibrosis transmembrane conductance regulator (CFTR) mutants (33) or NKCC2 mutants that cause Bartter syndrome. In the latter it was initially shown that Bartter syndrome mutants of NKCC2 could be trafficked to the membranes of *Xenopus* oocytes, although they remained non-functional (34). However, more recently it has been shown that in mammalian cells some Bartter syndrome mutants never leave the endoplasmic reticulum due to the absence of a trafficking signal in their C terminus (35). So, even though many proteins are trafficked similarly in *Xenopus* oocytes and mammalian cells, it is clear that some mutant transport proteins reach the surface of *Xenopus* oocytes, whereas they are not trafficked to the surface of mammalian cells. It is also possible that the NKCC2AF protein has a role at the cell surface in shark kidney (and is trafficked in *Xenopus* oocytes) that has been lost in mammals perhaps coinciding with the emergence of NKCC2B (5). The role of NKCC2AF in the mammalian kidney remains a mystery. Even though significant levels of NKCC2AF mRNA are present (2, 23), it is not known whether the protein is expressed or reaches the plasma membrane as current antibodies do not have the required selectivity. One possibility is that the mRNA is produced as a consequence of pre-mRNA splicing during regulation of expression of NKCC2A and -F.

Cross-linking studies of human NKCC2 expressed in *Xenopus* oocytes suggest that NKCC2 exists as a dimer in the membrane (36). Without making any attempt to stabilize dimers, Western blots (Fig. 2*B*) prepared from cells expressing all variants of fNKCC2 show a significant portion of the protein running at molecular weights consistent with the formation of dimers (Figs. 2, 3, and 5). In addition, the vast majority of fNKCC2A and -AF run at a high molecular weight on two-dimensional gel electrophoresis (Fig. 7). Again the weights are consistent with dimer formation, although we cannot rule out at this stage that a different protein is the binding partner(s). NKCC1 can also form dimers (37, 38) and the interaction appears to involve domains in the C terminus if the protein (39, 40), a region that is highly conserved in NKCC2. The question therefore arises whether NKCC1 can form heterodimers with NKCC2. Experiments based on yeast two-hybrid studies suggest they can (22), whereas pulldown assays using chimeric proteins suggest they do not (40). The regions in the C termini of NKCC2 involved in dimer formation are common to all variants (22). Our two-dimensional gel electrophoresis experiments show that co-expression of fNKCC2A or -AF with NKCC1 has no effect on the distribution of NKCC1 along a pH gradient (Fig. 7). Had there been significant NKCC1–fNKCC2 heterodimer formation the high molecular weight complexes detected by N1 should have moved in the alkaline direction (especially with fNKCC2AF). Our flux studies further support the notion that the isoforms do not interact. Expression of nonfunctional NKCC1 constructs in HEK-293 cells often substantially inhibit the activity of endogenous NKCC1 (12, 26). We have yet to find an NKCC2 construct whose expression affects endogenous NKCC1 activity. If the dominant-negative effect is mediated by dimer formation then it is unlikely that NKCC1 forms heterodimers with NKCC2. Perhaps the motifs that target the different isoforms to the apical or basolateral membranes also prevent such interactions.

A key issue in these studies was the choice of antibody to detect NKCC2. Initially we used antibodies raised to short peptides in the C or N termini of the transporter (Table 1). These antibodies detected bands at a high molecular mass (275 kDa), well above the expected monomeric mass (Fig. 2). Only L224 detected bands at the monomeric weight, and those were very weak. T4, a monoclonal antibody raised to a large section of the C terminus of NKCC1 and reacting with both NKCC isoforms, also only detected the high molecular weight forms. However, we found that phospho-specific antibodies were raised to epitopes in the N terminus of NKCC1 and conserved between NKCC isoforms, detected strong bands at the monomeric weight of NKCC2. Thus monomeric and high molecular weight forms of NKCC2 appear to have different structures that affect access of antibodies to their epitopes. These structural differences are maintained even though proteins have been treated with SDS sample buffer. Thus the transporter, expressed in HEK-293 cells, appears in a more closed state when monomeric and in a more open state when in high molecular weight forms. However, these same antibodies do detect some monomeric NKCC2 in kidney lysates (but far more high molecular weight

complexes). This may be due to the very high expression levels or may indicate that NKCC2 adopts a different conformation in its native environment. If true, this might also explain why the transporter is highly active in the kidney yet produces relatively small fluxes in transfected cells (Figs. 4 and 5). Reliable identification of NKCC2 becomes simplified with the development of a polyclonal antibody to the whole N terminus of NKCC2 (anti-NKCC2, Alessi, Dundee). This antibody detects all fNKCC2 variants at the expected monomeric weight as well as the high molecular weight forms. A slight drawback is its weak cross-reactivity with NKCC1, which must be taken into account when NKCC1 is overexpressed or when long exposures are used for detection. Anti-NKCC2 also detected strong monomeric bands in kidney lysates (Fig. 2*C*). It appears that antipeptide antibodies and monoclonal T4, all of which bind to small regions in the N and C termini of NKCC2, react almost exclusively with the high molecular weight forms despite the presence of significant amounts of monomers in the samples. Polyclonals to large domains seem more effective at recognizing the monomers. It was also noted that PNGase-treated fNKCC2 migrates substantially faster on SDS-PAGE than expected (~99 *versus* 121 kDa). This is not uncommon for membrane proteins as their SDS binding capacity can change with protein folding (41).

Relatively small bumetanide-sensitive ^{86}Rb fluxes were measured in HEK-293 cells transfected with fNKCC2 variants under basal conditions. A similar phenomenon occurs with cells stably expressing NKCC1. Here fluxes are barely larger than in untransfected controls, suggesting transfected cells switch off the expressed transporter. The presence of the functional transporter is only revealed if it can be reactivated. This can be achieved for NKCC1 by preincubating cells in a hypotonic/low-chloride medium that increases fluxes manyfold above background (6). However, this protocol only increases fluxes 2–3-fold in cells expressing fNKCC2, and background fluxes are stimulated to a greater extent. Our data thus suggest that NKCC2 is less responsive to changes in cell chloride concentration than NKCC1, and that the maneuver that helps reveal the presence of transfected NKCC1 in fact obscures the presence of transfected NKCC2. A more effective means of activating this transporter needs to be devised bearing in mind the possibility that HEK-293 cells may not express a necessary cofactor that is present in the native thick ascending limb of the Henle loop. Our work suggests that little is to be gained from increasing still further the phosphorylation of regulatory domain threonines and maneuvers that increase cell surface expression may provide a way forward. Although *Xenopus* oocytes prove useful for studying the biophysical properties of NKCC2, discrepancies in the behavior of NKCC2AF in *Xenopus* oocytes and HEK-293 cells highlight the importance of studying certain aspects of the regulation of NKCC2, especially those involving NKCC2 trafficking, in a mammalian expression system. The availability of stable NKCC2 cell lines should prove a useful tool in this endeavor.

Acknowledgments—We thank Professors D. Alessi, B. Forbush, and M. Knepper for the generous gifts of antibodies, Professor D. Alessi and Dr. Ciaran Richardson for helpful discussions.

REFERENCES

1. Gamba, G. (2005) *Physiol. Rev.* **85,** 423–493
2. Castrop, H., and Schnermann, J. (2008) *Am. J. Physiol. Renal Physiol.* **295,** F859–F866
3. Flatman, P. W. (2007) *Clin. Sci.* **112,** 203–216
4. Payne, J. A., and Forbush, B., 3rd (1994) *Proc. Natl. Acad. Sci. U.S.A.* **91,** 4544–4548
5. Gagnon, E., Forbush, B., Flemmer, A. W., Giménez, I., Caron, L., and Isenring, P. (2002) *Am. J. Physiol. Renal Physiol.* **283,** F1046–F1055
6. Isenring, P., Jacoby, S. C., Payne, J. A., and Forbush, B., 3rd (1998) *J. Biol. Chem.* **273,** 11295–11301
7. Benziane, B., Demaretz, S., Defontaine, N., Zaarour, N., Cheval, L., Bourgeois, S., Klein, C., Froissart, M., Blanchard, A., Paillard, M., Gamba, G., Houillier, P., and Laghmani, K. (2007) *J. Biol. Chem.* **282,** 33817–33830
8. Giménez, I., Isenring, P., and Forbush, B. (2002) *J. Biol. Chem.* **277,** 8767–8770
9. Plata, C., Meade, P., Vazquez, N., Hebert, S. C., and Gamba, G. (2002) *J. Biol. Chem.* **277,** 11004–11012
10. Gagnon, E., Bergeron, M. J., Daigle, N. D., Lefoll, M. H., and Isenring, P. (2005) *J. Biol. Chem.* **280,** 32555–32563
11. Giménez, I., and Forbush, B. (2007) *J. Biol. Chem.* **282,** 6540–6547
12. Darman, R. B., and Forbush, B. (2002) *J. Biol. Chem.* **277,** 37542–37550
13. Vitari, A. C., Thastrup, J., Rafiqi, F. H., Deak, M., Morrice, N. A., Karlsson, H. K., and Alessi, D. R. (2006) *Biochem. J.* **397,** 223–231
14. Lytle, C., and Forbush, B., 3rd (1996) *Am. J. Physiol.* **270,** C437–C448
15. Piechotta, K., Lu, J., and Delpire, E. (2002) *J. Biol. Chem.* **277,** 50812–50819
16. Dowd, B. F., and Forbush, B. (2003) *J. Biol. Chem.* **278,** 27347–27353
17. Giménez, I., and Forbush, B. (2005) *Am. J. Physiol. Renal Physiol.* **289,** F1341–F1345
18. Ponce-Coria, J., San-Cristobal, P., Kahle, K. T., Vazquez, N., Pacheco-Alvarez, D., de Los Heros, P., Juárez, P., Muñoz, E., Michel, G., Bobadilla, N. A., Gimenez, I., Lifton, R. P., Hebert, S. C., and Gamba, G. (2008) *Proc. Natl. Acad. Sci. U.S.A.* **105,** 8458–8463
19. Giménez, I., and Forbush, B. (2003) *J. Biol. Chem.* **278,** 26946–26951
20. Gamba, G., Miyanoshita, A., Lombardi, M., Lytton, J., Lee, W. S., Hediger, M. A., and Hebert, S. C. (1994) *J. Biol. Chem.* **269,** 17713–17722
21. Igarashi, P., Vanden Heuvel, G. B., Payne, J. A., and Forbush, B., 3rd (1995) *Am. J. Physiol.* **269,** F405–F418
22. Brunet, G. M., Gagnon, E., Simard, C. F., Daigle, N. D., Caron, L., Noël, M., Lefoll, M. H., Bergeron, M. J., and Isenring, P. (2005) *J. Gen. Physiol.* **126,** 325–337
23. Yang, T., Huang, Y. G., Singh, I., Schnermann, J., and Briggs, J. P. (1996) *Am. J. Physiol.* **271,** F931–F939
24. Oppermann, M., Mizel, D., Huang, G., Li, C., Deng, C., Theilig, F., Bachmann, S., Briggs, J., Schnermann, J., and Castrop, H. (2006) *J. Am. Soc. Nephrol.* **17,** 2143–2152
25. Flatman, P. W. (2002) *Biochim. Biophys. Acta* **1566,** 140–151
26. Isenring, P., and Forbush, B., 3rd (1997) *J. Biol. Chem.* **272,** 24556–24562
27. Khoudoli, G. A., Porter, I. M., Blow, J. J., and Swedlow, J. R. (2004) *Proteome Sci.* **2,** 6
28. Paredes, A., Plata, C., Rivera, M., Moreno, E., Vázquez, N., Muñoz-Clares, R., Hebert, S. C., and Gamba, G. (2006) *Am. J. Physiol. Renal Physiol.* **290,** F1094–F1102
29. Darman, R. B., Flemmer, A., and Forbush, B. (2001) *J. Biol. Chem.* **276,** 34359–34362
30. Flemmer, A. W., Gimenez, I., Dowd, B. F., Darman, R. B., and Forbush, B. (2002) *J. Biol. Chem.* **277,** 37551–37558
31. Ares, G. R., Caceres, P., Alvarez-Leefmans, F. J., and Ortiz, P. A. (2008) *Am. J. Physiol. Renal Physiol.* **295,** F877–F887
32. Maglova, L. M., Crowe, W. E., and Russell, J. M. (2004) *Am. J. Physiol. Cell Physiol.* **286,** C1324–C1334
33. Denning, G. M., Anderson, M. P., Amara, J. F., Marshall, J., Smith, A. E., and Welsh, M. J. (1992) *Nature* **358,** 761–764
34. Starremans, P. G., Kersten, F. F., Knoers, N. V., van den Heuvel, L. P., and Bindels, R. J. M. (2003) *J. Am. Soc. Nephrol.* **14,** 1419–1426

35. Zaarour, N., Demaretz, S., Defontaine, N., Mordasini, D., and Laghmani, K. (2009) *J. Biol. Chem.* **284,** 21752–21764
36. Starremans, P. G., Kersten, F. F., van den Heuvel, L. P., Knoers, N. V., and Bindels, R. J. (2003) *J. Am. Soc. Nephrol.* **14,** 3039–3046
37. Moore-Hoon, M. L., and Turner, R. J. (1998) *Biochim. Biophys. Acta* **1373,** 261–269
38. Matskevich, I., Hegney, K. L., and Flatman, P. W. (2005) *BBA Biomembranes* **1714,** 25–34
39. Simard, C. F., Brunet, G. M., Daigle, N. D., Montminy, V., Caron, L., and Isenring, P. (2004) *J. Biol. Chem.* **279,** 40769–40777
40. Parvin, M. N., Gerelsaikhan, T., and Turner, R. J. (2007) *Biochemistry* **46,** 9630–9637
41. Rath, A., Glibowicka, M., Nadeau, V. G., Chen, G., and Deber, C. M. (2009) *Proc. Natl. Acad. Sci. U.S.A.* **106,** 1760–1765